

## Crystallographic, thermodynamic, and transport properties of the $\text{Bi}_2\text{Sr}_{3-x}\text{Ca}_x\text{Cu}_2\text{O}_{8+\delta}$ superconductor

G. S. Grader, E. M. Gyorgy, P. K. Gallagher, H. M. O'Bryan, D. W. Johnson, Jr.,  
S. Sunshine, S. M. Zahurak, S. Jin, and R. C. Sherwood  
*AT&T Bell Laboratories, Murray Hill, New Jersey 07974*

(Received 21 March 1988)

We have demonstrated the presence of a single-phase solid solution for the  $\text{Bi}_2\text{Sr}_{3-x}\text{Ca}_x\text{Cu}_2\text{O}_{8+\delta}$  superconductor, in the  $1.25 \leq x \leq 2.0$  range. The lattice parameters and melting points vary monotonically with  $x$ , both increasing towards the Sr-rich composition. This monotonic variation of the lattice parameters extends into the  $0.8 \leq x \leq 2.2$  range, but the material is multiphased outside the  $1.25 \leq x \leq 2.0$  limit. Superconducting onsets in the ranges of 70–89 and 108–118 K have been obtained; however, the exact results are very sensitive to processing parameters. Magnetization measurements indicate high intragranular current densities ( $J_c$ ) at 5 K of  $\sim 5 \times 10^6$  A/cm<sup>2</sup>. The actual transport  $J_c$  is low ( $\approx 70$  A/cm<sup>2</sup> at 4 K) and exhibits a strong field dependence similar to the behavior of the  $\text{YBa}_2\text{Cu}_3\text{O}_7$  superconductor.

Following the discovery of superconductivity in the Bi-Sr-Ca-Cu-O system,<sup>1</sup> the identification of the superconducting phase<sup>2–5</sup> raised the possibility that Bi, Ca, and Sr form a solid solution  $\text{Bi}_2(\text{BiSrCa})_3\text{Cu}_2\text{O}_{8+\delta}$  in this material. In an earlier report,<sup>4</sup> single-phase material of the  $\text{Bi}_2\text{Sr}_{3-x}\text{Ca}_x\text{Cu}_2\text{O}_{8.13}$  composition was obtained in the  $1.25 \leq x \leq 1.75$  range. However, the expected continuous change in the lattice parameters with composition (due to the different Sr and Ca ionic radii), was not observed. The purpose of this work was first to demonstrate the presence of a Sr-Ca solid solution, and second to measure some of its thermodynamic and transport properties.

### MATERIALS PREPARATION

The samples for this study were prepared from nitrate precursors. Stock solutions of the Bi, Ca, and Cu salts were made by dissolving the nitrates in dilute nitric acid while  $\text{SrNO}_3$  was dissolved in water. The desired compositions were mixed by volume, and then spray-dried using a Büchi mini spray dryer. The effluent gas stream from the dryer (containing particles  $\approx 10$   $\mu\text{m}$  in diameter), was directed into a heated quartz tube in which turbulence was induced by a baffle. The turbulence enhanced the deposition of the particles on the furnace walls, where decomposition of the nitrates occurred. When a desired amount of material was collected, the quartz tube was removed and the powder scraped off the furnace walls. On a laboratory scale, this technique can generate 1–2 g of calcined, highly homogeneous material in about 20 min.

### CRYSTALLOGRAPHIC AND THERMODYNAMIC DATA

The existence of the solid solution  $\text{Bi}_2\text{Sr}_{3-x}\text{Ca}_x\text{Cu}_2\text{O}_{8+\delta}$  can be shown unambiguously by measuring the lattice parameters as a function of  $x$ . Lattice parameters of the Bi-Sr-Ca-Cu-O system were obtained by fitting x-ray

powder diffraction patterns using Cu  $K\alpha$  radiation to a tetragonal unit cell. A plot of the  $a$  and  $c$  axes as well as the computed unit-cell volume are shown in Fig. 1. As shown, in the  $0.8 \leq x \leq 2.2$  range the lattice parameters and cell volume increase monotonically towards the Sr-rich composition consistent with the larger Sr ionic radius. Single-phase material was obtained only in the  $1.25 \leq$

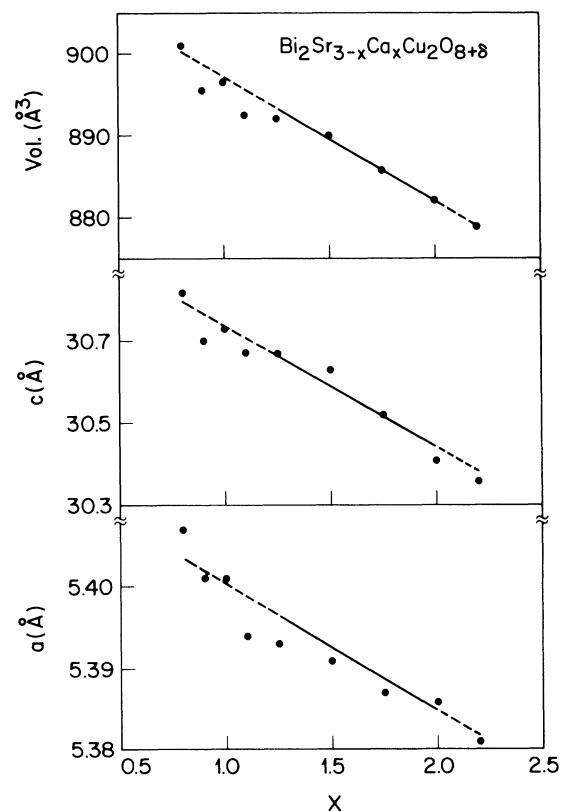


FIG. 1. The  $a$  and  $c$  lattice parameters and unit-cell volume of  $\text{Bi}_2\text{Sr}_{3-x}\text{Ca}_x\text{Cu}_2\text{O}_{8+\delta}$  as a function of  $x$ .

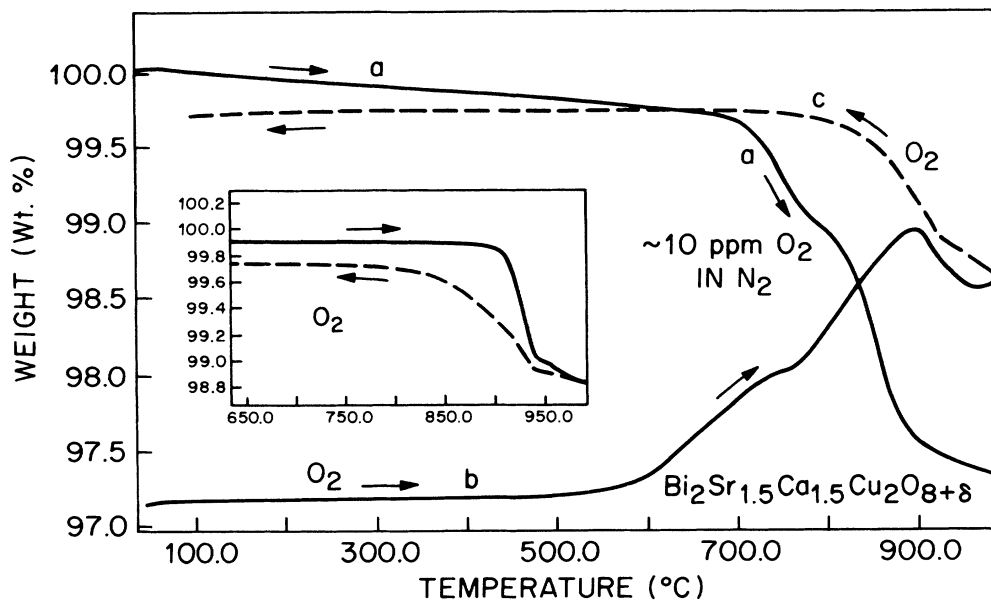


FIG. 2. Thermogravimetry (TG) of  $\text{Bi}_2\text{Sr}_{1.5}\text{Ca}_{1.5}\text{Cu}_2\text{O}_{8+\delta}$  at  $2^\circ\text{C min}^{-1}$  in oxygen and approximately 10 ppm  $\text{O}_2$  in  $\text{N}_2$ .

$x \leq 2.0$  range. The processing temperature ranged from 885 to 840°C for the  $x = 1.25$  to  $x = 2.0$  compositions, respectively. Above the  $x = 2.0$  limit some  $\text{Ca}_2\text{CuO}_3$  was present, while below  $x = 1.25$  a distinct set of peaks near  $2\theta = 30^\circ$  became apparent. The amount of these extra phases depends strongly on the processing temperature; thus, the exact value of  $x$  outside the  $1.25 \leq x \leq 2.0$  range is unclear. The continuous variation of the lattice parameters beyond the single-phase region, shown by the dotted lines in Fig. 1, may indicate that the solid solution can exist outside the  $1.25 \leq x \leq 2.0$  range. Materials prepared at the compositions  $x = 0.6$  and  $x = 2.5$  did not have the characteristic x-ray pattern of the superconducting phase, implying that the solid solution definitely does not exist at these compositions.

The melting point and oxygen contents of the samples were obtained from differential thermal analysis (DTA), and thermogravimetric (TG) data. The TG curve for  $\text{Bi}_2\text{Sr}_{1.5}\text{Ca}_{1.5}\text{Cu}_2\text{O}_{8+\delta}$  is shown in Fig. 2. The inset in Fig. 2 shows the heating and cooling of a sample in oxygen. The oxygen loss starts at  $\approx 900^\circ\text{C}$ ; not all the oxygen is picked up in the cooling stage possibly due to a partial decomposition and perhaps evaporation of some bismuth. A sample was then heated in  $\approx 10$  ppm  $\text{O}_2$  (curve *a*), where oxygen loss begins at  $\approx 700^\circ\text{C}$ . Upon cooling, the weight remained constant since no oxygen was added. The oxygen-deficient sample was then reheated and cooled in oxygen and most of the initial weight was regained (curves *b* and *c*). Both the loss and gain of oxygen appear to occur in a stepwise manner. The loss in nitrogen is about 2.5 greater than that in oxygen at  $980^\circ\text{C}$ . Depending upon the actual value of  $\delta$  in the starting material this corresponds to a loss of about 0.5–1.4 atoms of oxygen per formula weight, respectively.

Determination of the oxygen content of the samples by reduction in hydrogen is more difficult for these materials as compared with the Y-Ba-Cu-O system due to the rela-

tively high vapor pressure of Bi above  $\approx 700^\circ\text{C}$ . Preliminary results show that the oxygen content is significantly greater than 8.0 atoms per unit cell throughout the solid solution range. This implies either the presence of some  $\text{Cu}^{+3}$  ions,<sup>3,4</sup> or as claimed for the  $\text{YBa}_2\text{Cu}_3\text{O}_7$  system, the presence of  $\text{O}^{1-}$  ions.<sup>6,7</sup>

The melting point of the materials is readily obtained from DTA data. The variation of the melting point as a function of composition, determined from the extrapolated onset of the melting endotherm at  $10^\circ\text{C min}^{-1}$ , is shown in Fig. 3, for high and low oxygen pressures. The melting point decreases monotonically towards the calcium rich end. The oxygen pressure dependence of the melting point suggests that by processing the material at oxygen pressures  $> 1$  atmosphere, the melting temperature can be raised above  $900^\circ\text{C}$ . It may also be that the

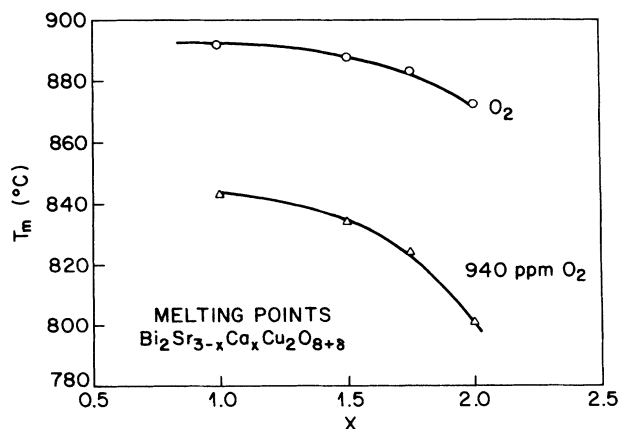


FIG. 3. The melting temperature of  $\text{Bi}_2\text{Sr}_{3-x}\text{Ca}_x\text{Cu}_2\text{O}_{8+\delta}$  as a function of  $x$ , in  $\text{O}_2$  and approximately 940 ppm  $\text{O}_2$  in  $\text{N}_2$ , respectively.

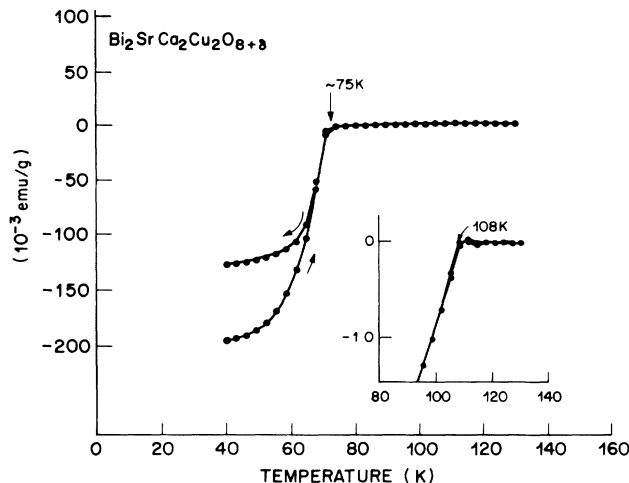


FIG. 4. Diamagnetic and Meissner effects of  $\text{Bi}_2\text{SrCa}_2\text{Cu}_2\text{O}_{8+\delta}$  using a squid magnetometer. The inset shows the onset of the transition above 100 K.

reactivity can be enhanced by initially firing in a low oxygen pressure to increase ionic mobilities, and then at a higher oxygen pressure to achieve proper oxidation.

#### MAGNETIC AND TRANSPORT DATA

The Meissner and diamagnetic effects were measured with a SQUID magnetometer (Quantum Design). Samples were first cooled in zero field, the field was then set to 20 Oe and the diamagnetic effect was recorded by heating to 130 K. The sample was then cooled in the presence of the field to record the Meissner effect. An example of such a trace is shown in Fig. 4 for the  $\text{Bi}_2\text{SrCa}_2\text{Cu}_2\text{O}_{8+\delta}$  composition processed at  $860^\circ\text{C}$  for 4 h. Based on the sample size, the diamagnetic signal at 40 K implies that  $\approx 70\%$  of the material is superconducting. The inset in Fig. 3 shows the onset of the high-temperature transition. It should be pointed out that although significant resistivity changes above 100 K are observed routinely, we have not yet obtained pronounced Meissner signals above 100 K, as reported elsewhere.<sup>4</sup> Superconducting onsets in the ranges of 70–89 K and 108–118 K have been obtained; however, the exact results are very sensitive to the processing parameters. The highest onsets have been obtained from partially melted samples, hence, the exact composition is unknown. Further work to clarify the issue is currently underway.

The magnetization of the samples was measured using a vibrating sample magnetometer (VSM). Data taken on a bulk piece of the  $\text{Bi}_2\text{Sr}_2\text{CaCu}_2\text{O}_{8+\delta}$  composition at  $\approx 5$  K, and on the same weight of a ground powder sample,

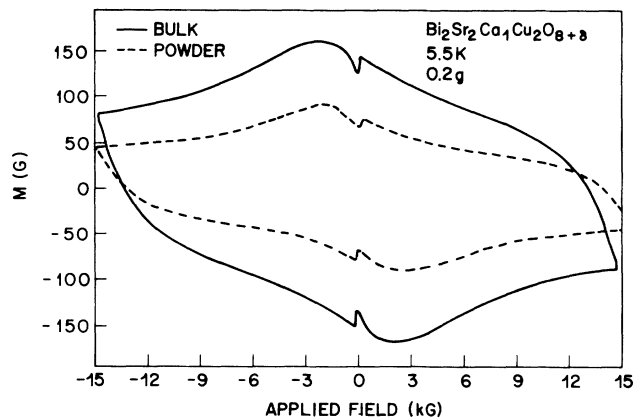


FIG. 5.  $M$ - $H$  loops of  $\text{Bi}_2\text{Sr}_2\text{CaCu}_2\text{O}_{8+\delta}$  using a vibrating sample magnetometer. The solid curve is for a bulk sample while the dashed curve is the powdered material.

are shown by the solid and dotted curves in Fig. 5, respectively. Since the magnetization curves in the two measurements are insignificantly different (by a factor of only about 2), the signal arises from currents within the individual grains in the material (the difference in the two measurements could arise from a reduction in the average grain size during the crushing). Based on an average grain size of  $\approx 10 \mu\text{m}$ , the critical current  $J_c$  within the grains is  $\approx 5 \times 10^6 \text{ A/cm}^2$  at 5 K (at a field of 9 kG). This result is consistent with recent transport measurements on thin epitaxial films of the Bi-Sr-Ca-Cu-O compound,<sup>8</sup> as well as with VSM measurements on single crystals.<sup>9</sup>

Just as in the  $\text{YBa}_2\text{Cu}_3\text{O}_7$  superconductor, the high intragranular  $J_c$  is not reproduced in bulk transport measurements, most likely due to weak links along grain boundaries. A transport measurement on the  $\text{Bi}_2\text{Sr}_2\text{CaCu}_2\text{O}_{8+\delta}$  composition (processed at  $890^\circ\text{C}$  for 8 h) at 4 K indicates a low  $J_c$  of about  $\approx 70 \text{ A/cm}^2$  in zero field. At a magnetic field of 100 G,  $J_c$  drops by about a factor of 2. Removal of the field and remeasurement of the critical current shows memory effect similar to that observed in the Ba-Y-Cu-O system.<sup>10</sup> Measurements of transport  $J_c$  at 77 K from a similar  $\text{Bi}_2\text{Sr}_2\text{CaCu}_2\text{O}_{8+\delta}$  compound showed a  $J_c$  of  $\approx 5 \text{ A/cm}^2$  in zero field, and strong field dependence ( $0.1 \text{ A/cm}^2$  at  $H=1000 \text{ G}$ ). Further research is required to understand the cause of the low  $J_c$  and the severe field dependence (“weak-link” problem) in this system.

#### ACKNOWLEDGMENT

The authors would like to thank D. W. Murphy for helpful discussions.

<sup>1</sup>H. Maeda, Y. Tanaka, M. Fukutomi, and T. Asano, *Jpn. J. Appl. Phys. Lett.* **27**, L209 (1988).

<sup>2</sup>R. M. Hazen, C. T. Prewitt, R. J. Angel, N. L. Ross, L. W. Finger, C. G. Hadjidakos, D. R. Veblen, P. J. Heaney, P. H.

Hor, R. L. Meng, Y. Y. Sum, Y. Q. Wang, Y. Y. Xue, Z. J. Huang, L. Gao, J. Bechtold, and C. W. Chu, *Phys. Rev. Lett.* **60**, 1174 (1988).

<sup>3</sup>S. A. Sunshine, T. Siegrist, L. F. Schneemeyer, D. W. Murphy,

- R. J. Cava, B. Batlogg, R. B. van Dover, R. M. Fleming, S. H. Glarum, S. Nakahara, R. Farrow, J. J. Krajewski, S. M. Zahurak, J. V. Waszczak, J. H. Marshall, P. Marsh, L. W. Rupp, Jr., and W. F. Peck, this issue, *Phys. Rev. B* **38**, 893 (1988).
- <sup>4</sup>J. M. Tarascon, Y. Le Page, P. Barboux, B. G. Bagley, L. H. Greene, W. R. McKinnon, G. W. Hull, M. Giroud, and D. M. Hwang, *Phys. Rev. B* **37**, 9382 (1988).
- <sup>5</sup>M. A. Subramanian, C. C. Torardi, J. C. Calabrese, J. Gopalakrishnan, K. J. Morrissey, T. R. Askew, R. B. Flippen, U. Chowdhry, and A. W. Sleight, *Science* **239**, 1015 (1988).
- <sup>6</sup>Y. Guo, Jean-Marc Langlois, and W. A. Goddard III, *Science* **239**, 896 (1988).
- <sup>7</sup>G. S. Grader, P. K. Gallagher, and A. T. Fiory, this issue, *Phys. Rev. B* **38**, 844 (1988).
- <sup>8</sup>C. E. Rice, A. F. J. Levi, R. M. Fleming, P. Marsh, K. W. Baldwin, M. Anzlowar, A. E. White, K. T. Short, S. Nakahara, and H. L. Stormer, *Appl. Phys. Lett.* **52**, 1828 (1988).
- <sup>9</sup>R. B. van Dover, L. F. Schneemeyer, E. M. Gyorgy, and J. V. Waszczak, *Appl. Phys. Lett.* **52**, 1910 (1988).
- <sup>10</sup>E. M. Gyorgy, G. S. Grader, D. W. Johnson, Jr., L. C. Feldman, D. W. Murphy, W. W. Rhodes, R. E. Howard, P. M. Mankiewich, and J. Skocpol, *Appl. Phys. Lett.* **52**, 328 (1988).